

oxygenase was set up simultaneously.

After 1 h of stirring at 10–15 °C, both the product-generating and control incubations were acidified to pH 1 (by pH paper) with concentrated HCl. Each incubation was extracted with 4 × 50 mL of CH₂Cl₂. The organic extracts were combined and then filtered through cotton (to remove water). After rotary evaporation at water aspirator vacuum, residual solvents were removed on a vacuum line. The crude residues obtained in this manner from each incubation were analyzed by high-field ¹H NMR for the presence of phenylboronic acid starting material and the presence or absence of phenol. In ¹H NMR of the control, of the two substances of interest, only phenyl boronic acid and not a trace of phenol could be detected. On the other hand, in the ¹H NMR of the product-generating incubation, both phenylboronic acid and phenol could be detected in the ratio phenylboronic acid/phenol = 3.2:1.0. Silica gel TLC (25% ethyl acetate/benzene; visualization with ultraviolet light, phos-

phomolybdic acid/EtOH, *p*-anisaldehyde–H₂SO₄/EtOH) confirmed these results for the presence of phenylboronic acid (*R_f* = 0.36) and the presence or absence of phenol (*R_f* = 0.75).

Registry No. Cyclohexanone oxygenase, 52037-90-8; cyclohexanone, 108-94-1; phenylacetone, 103-79-7; 2-phenyl-1-ethanal, 122-78-1; butanal, 123-72-8; phenylboronic acid, 98-80-6; *n*-butylboronic acid, 4426-47-5; *n*-octylboronic acid, 28741-08-4; thiane, 1613-51-0; ethyl *p*-tolyl sulfide, 622-63-9; phenyl allyl sulfide, 5296-64-0; thiane sulfoxide, 4988-34-5; phenyl methyl selenide, 4346-64-9; phenyl allyl selenide, 14370-82-2; triethyl phosphite, 122-52-1; sodium iodide, 7681-82-5; *tert*-butyl hydroperoxide, 75-91-2; hydrogen peroxide, 7722-84-1; perbenzoic acid, 93-59-4; *m*-chloroperbenzoic acid, 937-14-4; trifluoroperacetic acid, 359-48-8; cyclohexyl methyl ketone, 823-76-7; acetophenone, 98-86-2; 1,4-thioxane, 15980-15-1; *N,N*-dimethylbenzylamine, 103-83-3.

Aggregate Morphology and Intermembrane Interaction of Synthetic Peptide Lipids Bearing Various Head Groups

Yukito Murakami,* Jun-ichi Kikuchi, Toshihiko Takaki, Katsuya Uchimura, and Akio Nakano

Contribution No. 730 from the Department of Organic Synthesis, Faculty of Engineering, Kyushu University, Fukuoka 812, Japan. Received May 7, 1984

Abstract: Peptide lipids bearing three different head groups, cationic N⁺C₅Ala2C_{*n*}, anionic (SO₃⁻)C₅Ala2C_{*n*}, and nonionic QC₅Ala2C_{*n*}, were prepared for the investigation of their aggregate morphology and intermembrane interaction between the ionic and nonionic lipid aggregates in aqueous media. Anionic lipids bearing the sulfonate head group, (SO₃⁻)C₅Ala2C_{*n*}, form primarily lamellar aggregates in the aqueous dispersion state, which are converted into double-walled bilayer vesicles upon sonication. In contrast with the ionic lipids, nonionic lipids bearing the quinoyl head group, QC₅Ala2C_{*n*}, form highly ordered network assemblies in the dispersion state in the neutral pH range, and the sonication of such aggregates afforded scattered cloudlike assemblies without formation of small bilayer vesicles. QC₅Ala2C_{*n*} behaves as a normal anionic lipid under conditions that the hydroxyl groups of the quinoyl moiety are deprotonated and forms multiwalled bilayer vesicles in the dispersion state. The morphological change of the nonlamellar network aggregates of QC₅Ala2C_{*n*} is induced by intermembrane interaction with ionic peptide lipids to afford the normal bilayer membranes. The present results obtained by turbidity and differential scanning calorimetry measurements strongly indicate that the morphological change is induced by the one-way intermembrane transfer of the ionic lipid molecules through the intervening aqueous phase and the rate-determining step is the diffusion of the ionic lipid molecules from the bilayer phase to the bulk aqueous phase.

Clarification of aggregate morphology of synthetic lipids and characterization of their intermolecular and intervesicular interactions in aqueous media are indispensable not only for understanding physicochemical functions of biological membranes but also for developing membrane-mimetic reaction media. To overcome complexities and chemical instabilities of naturally occurring membranes, a large number of membrane-forming lipids have been prepared.¹ Most of these synthetic lipids as well as natural ones tend to form thermodynamically stable bilayer aggregates. Meanwhile, nonbilayer aggregates such as the inverted hexagonal (H_{II}) phase are also found under certain conditions in natural systems, and these nonbilayer phases may well be involved in dynamic intermembrane interactions.² As regards model membranes, however, there are few studies to clarify the intrinsic factors which control the formation of bilayer and nonbilayer aggregates and their interconversions due to the lack of appropriate synthetic lipids. We have recently prepared a series of peptide lipids involving an amino acid residue interposed between a polar head moiety and an aliphatic double-chain segment.³ The lipids

are so designed as to constitute the hydrogen-belt domain upon formation of bilayer aggregates in the light of the concept, so-called tripartite structure having a hydrogen-belt domain, for biomembranes.⁴ The cationic and zwitterionic peptide lipids have been observed to form bilayer membranes (vesicles and/or lamellae) in the aqueous dispersion state which are subsequently converted into distinct single-compartment vesicles upon sonication.³ Such single-compartment vesicles once formed remain in the solution without significant morphological change for a reasonably prolonged period of time. In contrast, a nonionic lipid having the quinoyl group as its polar head forms nonlamellar network aggregates⁵ which undergo morphological change as induced by intermembrane interaction with cationic bilayer vesicles.⁶

In the present work, we have studied primarily on the following two subjects. Firstly, the correlation between the nature of head groups of lipids and the aggregate morphology is clarified by

(1) Fendler, J. H. "Membrane Mimetic Chemistry"; Wiley: New York, 1982; Chapters 6 and 12.

(2) (a) Luzzati, V. In "Biological Membranes"; Chapman, D., Ed.; Academic Press: New York, 1968; pp 71–123. (b) Seddon, J. M.; Cevc, G.; Marsh, D. *Biochemistry* 1983, 22, 1280–1289. (c) Quinn, P. J.; Williams, W. P. *Biochim. Biophys. Acta* 1983, 737, 223–266.

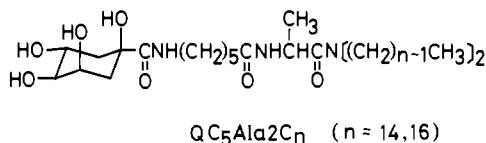
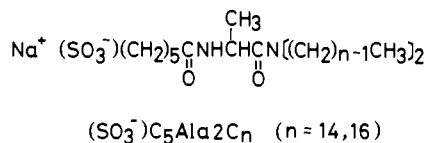
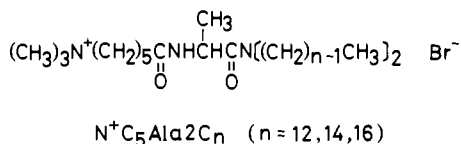
(3) (a) Murakami, Y.; Nakano, A.; Fukuya, K. *J. Am. Chem. Soc.* 1980, 102, 4253–4254. (b) Murakami, Y.; Nakano, A.; Ikeda, H. *J. Org. Chem.* 1982, 47, 2137–2144. (c) Murakami, Y.; Nakano, A.; Yoshimatsu, A.; Uchitomi, K.; Matsuda, Y. *J. Am. Chem. Soc.* 1984, 106, 3613–3623.

(4) Brockerhoff, H. In "Bioorganic Chemistry"; van Tamelen, E. E., Ed.; Academic Press: New York, 1977; Vol. 3, Chapter 1.

(5) In this article, "nonlamellar structure" was used for the aggregate morphology of QC₅Ala2C_{*n*} in aqueous media below pH 12.

(6) Murakami, Y.; Nakano, A.; Kikuchi, J.; Takaki, T.; Uchimura, K. *Chem. Lett.* 1983, 1891–1894.

employing cationic, anionic, and nonionic lipids; $N^+C_5Ala2C_n$, $(SO_3^-)C_5Ala2C_n$, and QC_5Ala2C_n , respectively. The L-alanine



residue was exclusively used an amino acid component which may constitute the hydrogen-belt domain upon formation of aggregates. Secondly, we demonstrate the morphological change of the nonlamellar network aggregates of QC_5Ala2C_n , as induced by intermembrane interaction with the ionic peptide lipids, $N^+C_5Ala2C_n$ and $(SO_3^-)C_5Ala2C_n$, resulting in the formation of normal bilayer membranes. The mechanism of such morphological change is to be discussed in light of turbidity and differential scanning calorimetry (DSC) data from the dynamic viewpoints.

Experimental Section

Materials. 1,6-Diphenyl-1,3,5-hexatriene (DPH) was obtained from Nakarai Chemicals as a guaranteed reagent and used without further purification. 6-((*tert*-Butoxycarbonyl)amino)hexanoic acid was prepared from 6-aminohexanoic acid and *O*-*tert*-butyl-*S*-(4,6-dimethyl-2-pyrimidinyl) thiocarbonate after the method of Nagasawa et al.⁷ *N,N*-Dihexadecyl-*N*^α-(*tert*-butoxycarbonyl)-L-alaninamide was obtained after the preparative method for *N,N*-didodecyl-*N*^α-(*tert*-butoxycarbonyl)-L-alaninamide, while *N,N*-ditetradecyl-*N*^α-(6-bromohexanoyl)-L-alaninamide and *N,N*-dihexadecyl-*N*^α-(6-bromohexanoyl)-L-alaninamide were synthesized after that for *N,N*-didodecyl-*N*^α-(6-bromohexanoyl)-L-alaninamide.^{3b} The preparation of cationic peptide lipids has been reported previously: *N,N*-didodecyl-*N*^α-[6-(trimethylammonio)hexanoyl]-L-alaninamide bromide ($N^+C_5Ala2C_{12}$),⁸ *N,N*-ditetradecyl-*N*^α-[6-(trimethylammonio)hexanoyl]-L-alaninamide bromide ($N^+C_5Ala2C_{14}$),^{3c} and *N,N*-dihexadecyl-*N*^α-[6-(trimethylammonio)hexanoyl]-L-alaninamide bromide ($N^+C_5Ala2C_{16}$).^{3c} *N,N*-Ditetradecyl-*N*^α-[6-(quinoylamino)hexanoyl]-L-alaninamide (QC_5Ala2C_{14}) was prepared according to a procedure similar to that adopted for the synthesis of QC_5Ala2C_{16} and characterized as reported elsewhere.⁶ The (-)-quinoyl moiety was introduced exclusively into both of the nonionic lipids.

N,N-Dihexadecyl-*N*^α-[6-((*tert*-butoxycarbonyl)amino)hexanoyl]-L-alaninamide ($BocNHC_5Ala2C_{16}$). Trifluoroacetic acid (25 g, 220 mmol) was added to a dry dichloromethane solution (40 mL) of *N,N*-dihexadecyl-*N*^α-(*tert*-butoxycarbonyl)-L-alaninamide (9.2 g, 16 mmol), and the mixture was stirred for 2 h at room temperature. Evaporation of an excess amount of trifluoroacetic acid in vacuo gave a pale brown oil. The amine thus formed was dissolved in chloroform (100 mL) and washed with 5% aqueous sodium hydrogen carbonate (3 × 40 mL). After being dried over sodium sulfate, the solution was evaporated in vacuo to give a pale yellow solid. Elimination of the *tert*-butoxycarbonyl group was confirmed by ¹H NMR spectroscopy. Dicyclohexylcarbodiimide (3.3 g, 16 mmol) was added to a solution of 6-((*tert*-butoxycarbonyl)amino)hexanoic acid (3.3 g, 15.2 mmol) in dry dichloromethane (50 mL) at 0 °C, followed by addition of the amine after 15 min. The mixture was stirred for 3 h at 0 °C and for 14 h at room temperature. The resulting precipitates (*N,N'*-dicyclohexylurea) were removed by filtration, the

solvent was evaporated in vacuo, and the residue was dissolved in ethyl acetate (150 mL). The solution was then washed with 10% aqueous citric acid (2 × 50 mL), water (50 mL), 4% aqueous sodium hydrogen carbonate (3 × 50 mL), and water (2 × 40 mL) in this sequence. After being dried over sodium sulfate, the solution was evaporated to dryness in vacuo. The residue was chromatographed on a column of silica gel (Wako gel C-100) with ethyl acetate as an eluant: a white solid, yield 10.4 g (quantitative); mp 40 °C; IR (neat) ν_{max} 3245 (NH str.), 2920 and 2840 (CH str.), 1720 and 1630 (C=O str.) cm^{-1} ; ¹H NMR ($CDCl_3$, Me_4Si) δ 0.89 [6 H, t, $(CH_2)_{15}CH_3$], 1.26 [65 H, m, $CH_2(CH_2)_{14}CH_3$, $CH(CH_3)$, and $CH_2(CH_2)_3CH_2CO$], 1.43 [9 H, s, $(CH_3)_3C$], 2.1 [2 H, t, CH_2CONH], 2.9–3.4 [6 H, m, $CONHCH_2$ and $NCH_2(CH_2)_{14}CH_3$], 4.8 [2 H, m, $CH(CH_3)$ and CH_2CONH], 6.41 [1 H, d, $CONH$].

N,N-Dihexadecyl-*N*^α-[6-((tetraacetylquinoyl)amino)hexanoyl]-L-alaninamide ($AcQC_5Ala2C_{16}$). Trifluoroacetic acid (25 g, 220 mmol) was added to a dry dichloromethane solution (60 mL) of $BocNHC_5Ala2C_{16}$ (7.2 g, 9.2 mmol), and the mixture was stirred for 2 h at room temperature. Evaporation of an excess amount of trifluoroacetic acid in vacuo gave a pale brown oil. Elimination of the *tert*-butoxycarbonyl group was confirmed by ¹H NMR spectroscopy. The amine was dissolved in dry dichloromethane (50 mL), and the solution was cooled to 0 °C. Triethylamine (10.0 g, 68 mmol) was added to the solution, and then (-)-tetraacetylquinoyl chloride⁹ (3.7 g, 9.6 mmol) dissolved in dry dichloromethane (20 mL) was added dropwise to the mixture at 0 °C with stirring. The resulting mixture was stirred for 3 h at room temperature and then washed with 4% aqueous sodium hydrogen carbonate (3 × 70 mL), water (70 mL), 5% aqueous citric acid (2 × 70 mL), and water (70 mL) in this sequence. After being dried over sodium sulfate, the solution was evaporated in vacuo to give a viscous pale yellow oil. The product was purified by gel-filtration chromatography on a column of Sephadex LH-20 with methanol as an eluant: a pale yellow solid, yield 6.8 g (74%); IR (neat) ν_{max} 3230 (NH str.), 1730 and 1620 (C=O str.) cm^{-1} ; ¹H NMR ($CDCl_3$, Me_4Si) δ 0.88 [6 H, t, $(CH_2)_{15}CH_3$], 1.27 [65 H, m, $CH_2(CH_2)_{14}CH_3$, $CH(CH_3)$, and $CH_2(CH_2)_3CH_2CO$], 2.0 [12 H, m, $OCOCH_3$], ~2.5 [2 H, m, CH_2CONH], 3.2 [10 H, m, $CONHCH_2$, $NCH_2(CH_2)_{14}CH_3$, and $CH_2CH(OCOCH_3)$], 4.6–5.7 [4 H, m, $CH(CH_3)$ and $CH(OCOCH_3)$], 6.12 [1 H, t, $CONHCH_2$], 6.60 [1 H, d, $CONHCH(CH_3)$].

N,N-Dihexadecyl-*N*^α-[6-(quinoylamino)hexanoyl]-L-alaninamide (QC_5Ala2C_{16}). After addition of hydrazine monohydrate (2.0 g, 40 mmol) to a solution of $AcQC_5Ala2C_{16}$ (2.0 g, 20 mmol) in 85% aqueous ethanol (20 mL), the mixture was refluxed for 1 h, cooled to room temperature, poured into cold water (200 mL), and extracted with chloroform (4 × 150 mL). After being dried over calcium sulfate, the solution was evaporated to dryness in vacuo. The residue was purified by gel-filtration chromatography on a column of Sephadex LH-20 with methanol as an eluant: a colorless solid, yield 252 mg (15%); $[\alpha]_D^{25} - 32^\circ$ (*c* 1.02, ethanol); IR (neat) ν_{max} 3300 (OH and NH str.), 1630 (C=O str.) cm^{-1} ; ¹H NMR ($CDCl_3$, Me_4Si) δ 0.93 [6 H, t, $(CH_2)_{15}CH_3$], 1.25 [65 H, m, $CH_2(CH_2)_{14}CH_3$, $CH(CH_3)$, and $CH_2(CH_2)_3CH_2CO$], ~2.5 [2 H, m, CH_2CONH], 2.9–3.6 [11 H, m, $CONHCH_2$, $NCH_2(CH_2)_{14}CH_3$, $CH_2CH(OH)$, and $CH(OH)CH(OH)CH(OH)$], 3.8–4.5 [2 H, m, $CH(OH)CH_2$], 4.75 [1 H, m, $CH(CH_3)$]. Anal. Calcd for $C_{48}H_{93}N_3O_5$: C, 69.99; H, 11.37; N, 5.10. Found: C, 69.67; H, 11.33; N, 5.10.

Sodium *N,N*-Ditetradecyl-*N*^α-(6-sulfohexanoyl)-L-alaninamide ($(SO_3^-)C_5Ala2C_{14}$). An aqueous solution (100 mL) of sodium sulfite (3.1 g, 29 mmol) was added dropwise to a solution of *N,N*-ditetradecyl-*N*^α-(6-bromohexanoyl)-L-alaninamide (1.8 g, 2.7 mmol) in ethanol (100 mL). The resulting mixture was refluxed for 234 h and cooled to room temperature. After an insoluble material was removed by filtration, the mixture was evaporated to dryness in vacuo. The residue was purified by gel-filtration chromatography on a column of Sephadex LH-20 with methanol as an eluant: a colorless solid, yield 0.40 g (22%); final mp 135 °C; $[\alpha]_D^{25} - 18.3^\circ$ (*c* 1.00, ethanol); IR (neat) ν_{max} 3210 (NH str.), 2920 and 2840 (CH str.), 1620 (C=O str.), 1190 and 1050 (SO_3^- str.) cm^{-1} ; ¹H NMR ($CDCl_3$, Me_4Si) δ 0.89 [6 H, t, $(CH_2)_{13}CH_3$], 1.27 [57 H, m, $CH_2(CH_2)_{12}CH_3$, $CH(CH_3)$, and $CH_2(CH_2)_3CH_2CO$], 2.21 [2 H, t, CH_2CO], 2.80 [2 H, t, $(SO_3^-)CH_2$], 3.28 [4 H, t, NCH_2], 4.80 [1 H, m, $CH(CH_3)$], 7.23 [1, H, d, $CONH$]. Anal. Calcd for $C_{37}H_{73}N_2NaO_5S \cdot 1/2H_2O$: C, 64.40; H, 10.81; N, 4.06. Found: C, 64.33; H, 10.72; N, 4.07.

Sodium *N,N*-Dihexadecyl-*N*^α-(6-sulfohexanoyl)-L-alaninamide ($(SO_3^-)C_5Ala2C_{16}$). This was prepared from *N,N*-dihexadecyl-*N*^α-(6-bromohexanoyl)-L-alaninamide in a manner similar to that stated above: a colorless solid, yield 18%; final mp 147 °C; $[\alpha]_D^{25} - 17.4^\circ$ (*c* 1.09, ethanol); IR (KBr disk) ν_{max} 3300 (NH str.), 2920 and 2850 (CH str.),

(7) Nagasawa, T.; Kuroiwa, K.; Narita, K.; Isowa, Y. *Bull. Chem. Soc. Jpn.* **1973**, *46*, 1269–1272.

(8) Murakami, Y.; Aoyama, Y.; Nakano, A.; Tada, T.; Fukuya, K. *J. Am. Chem. Soc.* **1981**, *103*, 3951–3953.

(9) Grewe, R.; Haendler, H. *Justus Liebig's Ann. Chem.* **1962**, *658*, 113–119.

1640 (C=O str.), 1190 and 1060 (SO_3^- str.) cm^{-1} ; $^1\text{H NMR}$ (CDCl_3 , Me_2Si) δ 0.87 [6 H, t, $(\text{CH}_2)_{15}\text{CH}_3$], 1.24 [65 H, m, $\text{CH}_2(\text{CH}_2)_{14}\text{CH}_3$, $\text{CH}(\text{CH}_3)$], and $\text{CH}_2(\text{CH}_2)_3\text{CH}_2\text{CO}$], 2.20 [2 H, m, CH_2CO], 2.89 [2 H, t, $(\text{SO}_3^-)\text{CH}_2$], 3.25 [4 H, t, NCH_2], 4.79 [1 H, m, $\text{CH}(\text{CH}_3)$], 7.29 [1 H, d, CONH]. Anal. Calcd for $\text{C}_{41}\text{H}_{81}\text{N}_2\text{NaO}_5\text{S} \cdot 1/2\text{H}_2\text{O}$: C, 66.00; H, 11.08; N, 3.75. Found: C, 66.19; H, 11.04; N, 3.82.

General Analyses and Measurements. Elemental analyses were performed at the Microanalysis Center of Kyushu University. Melting points were measured with a Yanagimoto MP-S1 apparatus (hot-plate type). $^1\text{H NMR}$ spectra were taken on a Hitachi R-24B or a Hitachi Perkin-Elmer R-20 spectrometer. IR spectra were recorded on a JASCO IR-E, a JASCO DS-403G grating, or a JEOL JIR-03F FT-IR spectrophotometer,¹⁰ cells of 0.1-mm path length with CaF_2 windows being used for solution samples. pH Measurements were carried out with a Beckman Φ 71 pH meter equipped with a Beckman 39505 combined electrode after calibration with a combination of appropriate standard aqueous buffers. Turbidity measurements were run at 400 nm on a Hitachi 340 or a Union Giken SM-401 high-sensitivity spectrophotometer with a cell of 0.1-mm path length.

Preparation of Membranes. The lipids dissolved individually in 1 mL of chloroform were dried in vacuo to give thin films. The resulting films in each 2 mL of water afforded aqueous dispersions by vortex mixing with glass beads at room temperature for 1–40 min. The corresponding ultrasonicated solutions of the lipids were prepared from the aqueous dispersions with a probe-type sonicator at 30 W (W-220F, Heat Systems-Ultrasonics) and allowed to stand at room temperature for 20 min.

Differential Scanning Calorimetry (DSC). Each 50- μL sample of an aqueous dispersion (2.5 mM) in redistilled and deionized water was weighed and sealed into a silver capsule. The phase transition temperature (T_m , temperature at a peak maximum of DSC thermogram) for an amphiphile was measured with a differential scanning calorimeter (Daini Seikosha SSC-560U): heating rate, 1 $^\circ\text{C}/\text{min}$; chart speed, 0.5 cm/min ; sensitivity, 0.029 mcal/s (full scale); temperature and transition heat calibrated with benzophenone (48 $^\circ\text{C}$) and/or water (0 $^\circ\text{C}$). The enthalpy change for phase transition (ΔH) was determined by measuring the peak area of the DSC thermogram.

Fluorescence Polarization. The fluorescence polarization measurements were carried out on a Union Giken FS-501A fluorescence polarization spectrophotometer equipped with a Sord microcomputer M200 Mark II; the emission at 450 nm originated from DPH was monitored upon excitation at 366 nm with a slit width of 3.5 nm for both excitation and emission sides. The steady-state fluorescence anisotropy (r_s) was calculated by eq 1, where I is the fluorescence intensity, and the sub-

$$r_s = (I_{vv} - C_f I_{vh}) / (I_{vv} + 2C_f I_{vh}) \quad (1)$$

scripts v and h refer to the orientations, vertical and horizontal, respectively, for the excitation and analyzer polarizers in this sequence; e.g., I_{vh} indicates the fluorescence intensity measured with a vertical excitation polarizer and a horizontal analyzer polarizer. C_f is the grating correction factor, given by I_{hv}/I_{hh} . The r_s value can be alternatively given by eq 2,¹¹

$$r_s = \frac{r_0 - r_\infty}{1 + (\tau/\phi)} + r_\infty \quad (2)$$

τ being the fluorescence lifetime, ϕ the rotational relaxation time, r_0 the maximal fluorescence anisotropy in the absence of any rotational motion, and r_∞ the limiting fluorescence anisotropy. The first term of eq 2 represents the kinetic component and is proportional to the microscopic viscosity, while the second term is the structural one and correlated with the membrane order parameter (S) by eq 3.¹² Recently, van Blitterswijk

$$r_\infty = r_0 S^2 \quad (3)$$

and his co-workers proposed a theoretical correlation between r_s and S for DPH in the membrane based on a theory of rotational dynamics in liquid crystals as given by eq 4, and the calculation was in good agree-

$$r_s = \frac{2(1 + 2S)(1 - S)(1 - S^2)}{20(1 + S) + 5(1 + 2S)(1 - S)} + \frac{2}{3} S^2 \quad (4)$$

$$0 < S \leq 1$$

ment with experimental data for artificial and biological membranes in

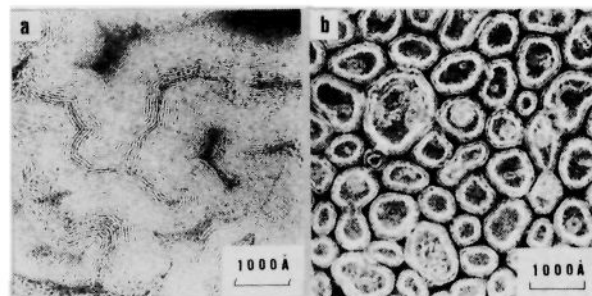


Figure 1. Electron micrographs for $(\text{SO}_3^-)\text{C}_5\text{Ala}2\text{C}_{14}$ negatively stained with uranyl acetate: (a) 5 mM aqueous dispersion, (b) 5 mM aqueous solution sonicated for 2 min at 30 W.

the range of $0.3 < S < 1$.¹³ In this work, we adopted eq 4 to evaluate the order parameter (S) from the steady-state fluorescence anisotropy of DPH embedded in membranes.

Electron Microscopy. Electron micrographs were obtained by means of negative staining and freeze-fracture techniques.¹⁴ The negatively stained samples were prepared as follows. An aqueous sample of lipid aggregates was applied on a carbon grid for 30 s, and the excess was blotted off. A 2% (w/w) aqueous solution of uranyl acetate was applied on it for 30 s, the excess was blotted off, and the resulting sample was dried in a vacuum desiccator at room temperature. As regards the freeze-fracture replica method with a Model FD-2A apparatus of Eiko Engineering Co., a sample solution placed on a sampling rod was frozen instantaneously upon its immersion in Freon 22 kept at -160 $^\circ\text{C}$. The frozen sample was fractured at -160 $^\circ\text{C}$ under 10^{-6} torr, and platinum metal and carbon were deposited on the rotating fractured surface. The specimen thus obtained was immersed in water-methanol (1:1 v/v) and washed, and the resulting replica was applied on a carbon grid. A JEOL JEM-200B electron microscope, installed at the Research Laboratory for High Voltage Electron Microscopy of Kyushu University, was used for the measurements.

Results and Discussion

Aggregate Morphology of Individual Lipids in Aqueous Media.

Cationic peptide lipids bearing the trimethylammonio moiety as the polar head group, $\text{N}^+\text{C}_5\text{Ala}2\text{C}_n$ ($n = 12, 14, 16$), form bilayer aggregates, multilayered vesicles and/or lamellae, when dispersed in aqueous media. These multilayered aggregates are converted into single-walled vesicles in aqueous media upon sonication as confirmed by electron microscopy.^{3c} In general, these single-walled vesicles are so stable that the fusion process is inhibited under ordinary conditions.^{3c} The morphological stability of these vesicles seems to be gained partly by the hydrogen-bonding interaction effective in the so-called hydrogen-belt domain in addition to the hydrophobic effect in the interior double-chain domain. Such a single-walled vesicle provides two different binding sites for hydrophobic substrates as separated by the hydrogen-belt barrier.^{7,15} To confirm the presence of the hydrogen-belt domain in the vesicles, the infrared spectra of $\text{N}^+\text{C}_5\text{Ala}2\text{C}_{14}$ were taken in various media with attention to the C=O stretching mode: 1% (w/w) in liquid paraffin, 1643 cm^{-1} ; 1% (w/w) in chloroform, 1632 cm^{-1} ; neat, 1622 cm^{-1} . These frequencies obviously reflect the extents of hydrogen-bonding interaction of the amide group.¹⁶ The FT-IR spectrum of the 1% (w/w) deuterium oxide solution of $\text{N}^+\text{C}_5\text{Ala}2\text{C}_{14}$ in the single-walled vesicular state showed the amide C=O stretching mode at 1624 cm^{-1} . This clearly indicates that the amide moieties of the vesicle build up the hydrogen-belt domain.

Anionic peptide lipids, $(\text{SO}_3^-)\text{C}_5\text{Ala}2\text{C}_n$ ($n = 14, 16$), afford multilayered aggregates, bent lamellae (Figure 1a) and vesicles, when dispersed in aqueous media. Sonication of the aqueous dispersion of $(\text{SO}_3^-)\text{C}_5\text{Ala}2\text{C}_{14}$ with a probe-type sonicator for

(10) The FT-IR spectra were measured by courtesy of Prof. I. Mochida of Kyushu University.

(11) Shinitzky, M.; Barenholz, Y. *Biochim. Biophys. Acta* **1978**, *515*, 367–394.

(12) (a) Heyn, M. P. *FEBS Lett.* **1979**, *108*, 359–364. (b) Jähnig, F. *Proc. Natl. Acad. Sci. U.S.A.* **1979**, *76*, 6361–6365.

(13) van Blitterswijk, W. J.; van Hoesen, R. P.; van der Meer, B. W. *Biochim. Biophys. Acta* **1981**, *644*, 323–332.

(14) The freeze-fracture replicas were prepared by courtesy of Prof. T. Kunitake of our department.

(15) Murakami, Y.; Nakano, A.; Yoshimatsu, A. *Chem. Lett.* **1984**, 13–16.

(16) Silverstein, R. M.; Bassler, G. C.; Morrill, T. C. "Spectrometric Identification of Organic Compounds"; Wiley: New York, 1981; Chapter 3.

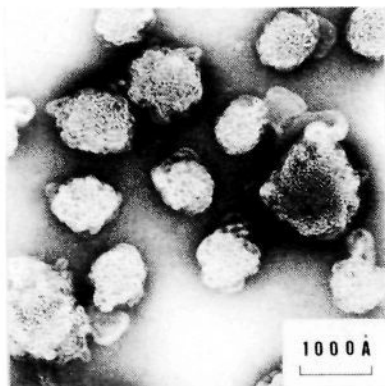


Figure 2. Electron micrograph for QC_5Ala2C_{14} negatively stained with uranyl acetate; 5 mM aqueous solution sonicated for 6 min at 30 W

2 min at a 30-W power level gave a clear solution, and its electron micrograph showed the presence of double-walled vesicles in the diameter range 200–800 Å (Figure 1b). The transformation into single-walled vesicles was not observed even after prolonged sonication (for 30 min at 30 W). The prevailing formation of the double-walled vesicles may primarily come from the increased effective bulkiness of the sulfonate group in the vesicular surface due to its solvation or mutual electrostatic repulsion, since the similar behavior was observed with cationic and zwitterionic peptide lipids bearing the bulky leucine residue(s).^{3b} On the other hand, an aqueous solution of $(SO_3^-)C_5Ala2C_{16}$ obtained by sonication for 10 min at 30 W was found to involve small particles in the diameter range 200–500 Å for which the internal aqueous compartment was not identified clearly. The similar morphology was observed for sonicated solutions of $N^+C_5Ala2C_n$ ($n \geq 16$).^{3c}

In contrast with the ionic peptide lipids, nonionic lipids bearing the quinoyl group, QC_5Ala2C_n ($n = 14, 16$), do not form ordinary bilayer aggregates in aqueous media. The negatively stained electron micrograph for an aqueous dispersion of QC_5Ala2C_{14} showed the presence of a highly ordered network assembly with a repeating distance of 70 Å that corresponds to the magnitude of the thickness of two lipid monolayers (ca. 40 Å) plus the diameter of an inner aqueous compartment (ca. 30 Å),⁶ the cross-sectional view of such aggregate being schematically shown in Figure 8. Multilayered vesicles and/or lamellae were not observed at all by electron microscopy, the negative staining and freeze-fracture techniques being employed for the aqueous dispersion. The formation of relatively small aqueous compartments (ca. 30-Å diameter), as compared with the inner water pool of single-walled vesicles (150–200-Å diameter), must primarily arise from an effective intermolecular hydrogen-bonding interaction between the hydroxyl groups in each polar domain. Sonication of the aqueous dispersion for 6 min at a 30-W power level gave a clear solution. However, the scattered cloudlike assemblies, which look like entangled aggregates of strings or tubes, were observed by electron microscopy without formation of small vesicles (Figure 2). The aggregate morphology of QC_5Ala2C_{16} in aqueous media is identical with that of QC_5Ala2C_{14} as confirmed by electron microscopy with the negative staining technique.

QC_5Ala2C_n ($n = 14, 16$) behaves as an anionic lipid in alkaline aqueous media under conditions that the hydroxyl groups of the quinoyl moiety are deprotonated. In the dispersion state at pH 13, QC_5Ala2C_{14} forms multiwalled bilayer vesicles in the diameter range 2500–5500 Å as observed in the freeze-fracture electron micrograph (Figure 3). Transformation of the network structure of the nonionic QC_5Ala2C_{14} aggregate into the normal bilayer membrane as pH was raised was reflected on a turbidity change in the dispersion state; the drastic decrease in turbidity at pH 12.5 (Figure 4) corresponds to the change in aggregate morphology upon deprotonation of the lipid.

It has been shown previously that for a lipid of optimal area a_0 , hydrocarbon volume v , and critical chain length l_c , the value of the dimensionless packing parameter $v/(a_0l_c)$ determines which aggregate structure is assumed.¹⁷ According to this concept, the

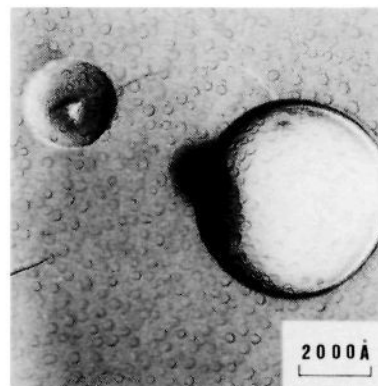


Figure 3. Freeze fracture electron micrograph for 10 mM aqueous dispersion of QC_5Ala2C_{14} at pH 13.0.

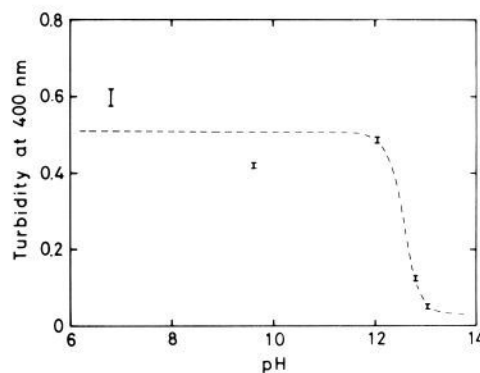


Figure 4. Correlation of turbidity with pH for 2.5 mM aqueous dispersion of QC_5Ala2C_{14} at 25.0 °C.

Table I. Phase Transition Parameters for Peptide Lipids in Aqueous Dispersion^a

peptide lipid	pH	$n = 14$		$n = 16$	
		T_m , °C	ΔH , kcal/mol	T_m , °C	ΔH , kcal/mol
$N^+C_5Ala2C_n$	7.0	2.0 ^b	4.9 ^b	25.5 ^b	7.8 ^b
$(SO_3^-)C_5Ala2C_n$	7.0	2.1	4.7	25.0	7.1
QC_5Ala2C_n	7.0	1.9	2.3	24.7 (24)	4.7
QC_5Ala2C_n	13.0	1.4	4.4	22.6 (22)	7.0

^a Evaluated by DSC, while the values in parentheses were determined by fluorescence polarization spectroscopy. ^b Taken from ref 3c.

nonlamellar structure observed with QC_5Ala2C_n is permitted when $v/(a_0l_c) > 1$, whereas the bilayer structures observed with other lipids are formed under the conditions $1/2 < v/(a_0l_c) < 1$. Molecular shapes of all the present peptide lipids having the same double alkyl chains are more or less comparable to each other in terms of v and l_c values, judging from their CPK molecular models. On the basis of the Ninham concept, the a_0 value primarily controls the aggregate morphology for the present synthetic lipids. In other words, the electrostatic repulsion between the charged head groups and hydration of them in the ionic vesicles give larger a_0 values than the intermolecular hydrogen-bonding interaction between the quinoyl groups in the QC_5Ala2C_n aggregates.

Phase Transition Behavior of Individual Lipid Aggregates. The phase transition parameters (maximum temperature, T_m ; enthalpy change, ΔH) of the aggregates formed with the present amphiphiles were measured in the dispersion state by DSC and are summarized in Table I. We have previously reported that the parameters (T_m and ΔH) for the cationic peptide lipids, $N^+C_5Ala2C_n$, are linearly correlated with the size of double-chain segment.^{3c} The parameters for the anionic bilayer aggregates

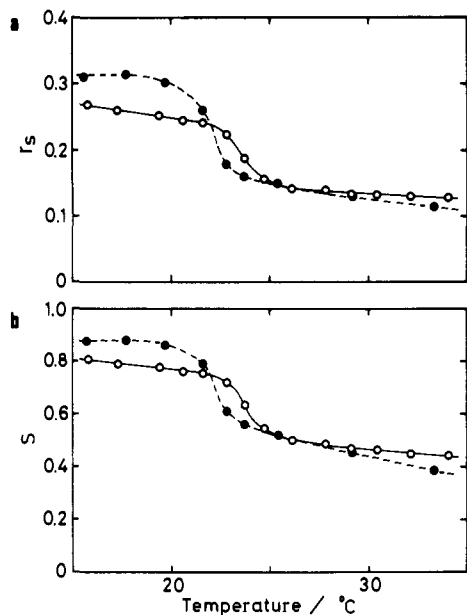


Figure 5. Correlations of temperature with (a) steady-state fluorescence anisotropy r_s and (b) order parameter S for DPH (1.0×10^{-7} M) embedded in aggregates of 1 mM QC_5Ala2C_{16} at pH 7.0 (O) and 13.0 (●).

composed of $(SO_3^-)C_5Ala2C_n$ ($n = 14, 16$) at pH 7 and QC_5Ala2C_n ($n = 14, 16$) at pH 13 are comparable to those for the cationic ones of $N^+C_5Ala2C_n$ ($n = 14, 16$) having the same double-chain segments. In other words, when the aggregate structures are comparable to each other among various lipids, the nature of the head group segments has little effect on the phase transition parameters.

The aggregates of QC_5Ala2C_n ($n = 14, 16$) at pH 7 exhibit smaller ΔH values relative to the corresponding values obtained at pH 13, while the T_m values are not much in variance. This implies that the molecular arrangement of hydrocarbon double chains in the gel state is more disordered in the neutral pH range than in the alkaline region. This idea was supported by fluorescence polarization spectroscopy. The steady-state fluorescence anisotropy (r_s) of 1,6-diphenyl-1,3,5-hexatriene (DPH) embedded in the aggregates of QC_5Ala2C_{16} at pH 7 and 13 was evaluated. Figure 5 shows the temperature dependence of the r_s value and the order parameter (S) calculated from r_s according to eq 4. The T_m values obtained from the inflection points (Figure 5) are in good agreement with those evaluated by DSC. The order parameters of the QC_5Ala2C_{16} aggregate at pH 7 are smaller than those at pH 13 in the gel state, while there is no significant difference between both aggregates at pH 7 and 13 in the liquid crystalline state above 25 °C. The temperature dependence of the order parameter for the multiwalled bilayer membrane of $N^+C_5Ala2C_{16}$ is quite comparable to that for the QC_5Ala2C_{16} aggregate at pH 13, S being 0.865 at 15.1 °C and 0.450 at 27.8 °C. This means that, in the gel state, the molecular packing mode in the hydrophobic domain of the QC_5Ala2C_{16} aggregate at pH 7 is more disordered than that of the multiwalled bilayer membranes. The result is consistent with the proposed structure for the QC_5Ala2C_{14} aggregate on the basis of electron microscopy.⁶

Intermembrane Interaction between Ionic and Nonionic Lipids.

In the previous communication,⁶ we have shown that the intermembrane lipid transfer between aggregates composed of $N^+C_5Ala2C_{16}$ and those of QC_5Ala2C_{14} induces the morphological change of individual aggregates and leads to the formation of smaller vesicles as confirmed by electron microscopy and DSC. In the present work, the effect of the double-chain length of each lipid on the rate of morphological change was investigated in aqueous media at pH 7. The transformation of the aggregate morphology of QC_5Ala2C_n into the normal bilayer membrane is reflected on turbidity of its aqueous dispersion. When an equimolar mixture of aqueous dispersions of $N^+C_5Ala2C_n$ ($n = 12,$

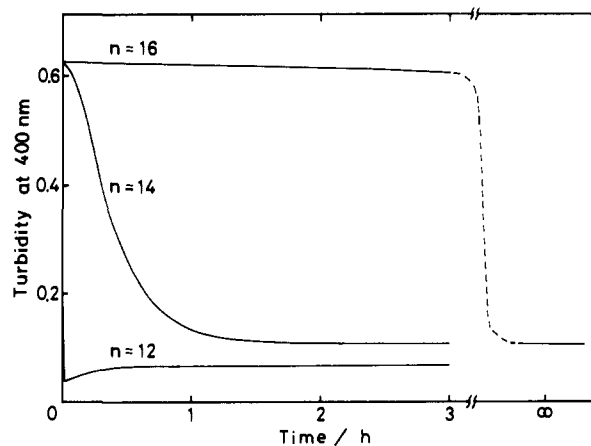


Figure 6. Time courses of turbidity change for equimolar mixtures of aqueous dispersions of $N^+C_5Ala2C_n$ ($n = 12, 14,$ and 16) and QC_5Ala2C_{16} (2.5 mM each) at pH 7.0 and 40.0 °C.

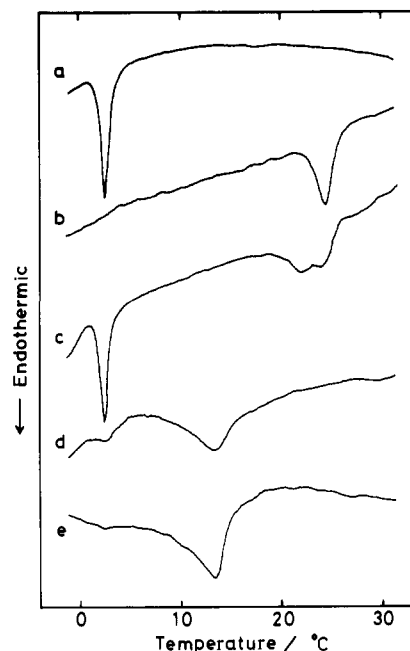


Figure 7. DSC thermograms for aqueous dispersions of peptide lipids: (a) $N^+C_5Ala2C_{14}$ (2.5 mM), (b) QC_5Ala2C_{16} (2.5 mM). An equimolar mixture of aqueous dispersions of $N^+C_5Ala2C_{14}$ and QC_5Ala2C_{16} (2.5 mM each) was incubated at pH 7.0 and 40.0 °C for the following periods of time: (c) immediately after mixing, (d) 20 min, and (e) 1 h; (e) being equivalent to the thermogram for a homogeneous mixture of $N^+C_5Ala2C_{14}$ and QC_5Ala2C_{16} (2.5 mM each).

14, 16) and QC_5Ala2C_n ($n = 14, 16$) (2.5 mM each) was incubated at 40.0 °C, the time course of the turbidity change at 400 nm was considerably dependent on the hydrocarbon chain length of the cationic lipids (Figure 6). The half times of turbidity change for combinations of the QC_5Ala2C_{16} aggregate with the $N^+C_5Ala2C_n$ membranes were ca. 10 s, 13 min, and 24 h, respectively, for $n = 12, 14,$ and 16 of the latter lipids. QC_5Ala2C_{16} can be replaced with QC_5Ala2C_{14} without change in the rate of turbidity decrease. When the single-walled vesicles of $N^+C_5Ala2C_n$ were incubated with the dispersion of QC_5Ala2C_n , the turbidity was reduced in a similar manner within the comparable time scale. Accordingly, the morphological state of the cationic lipids (multiwalled or single-walled vesicles or lamellae) scarcely gives out influence on the rate of morphological change. An addition of the multiwalled bilayer aggregates of $(SO_3^-)C_5Ala2C_{14}$ to the dispersion of QC_5Ala2C_{14} at pH 7 also resulted in the turbidity decrease at the rate (half time, 22 min) comparable to the $N^+C_5Ala2C_{14}$ - QC_5Ala2C_{14} system (half time, 19 min). This reveals that these systems undergo the morpho-

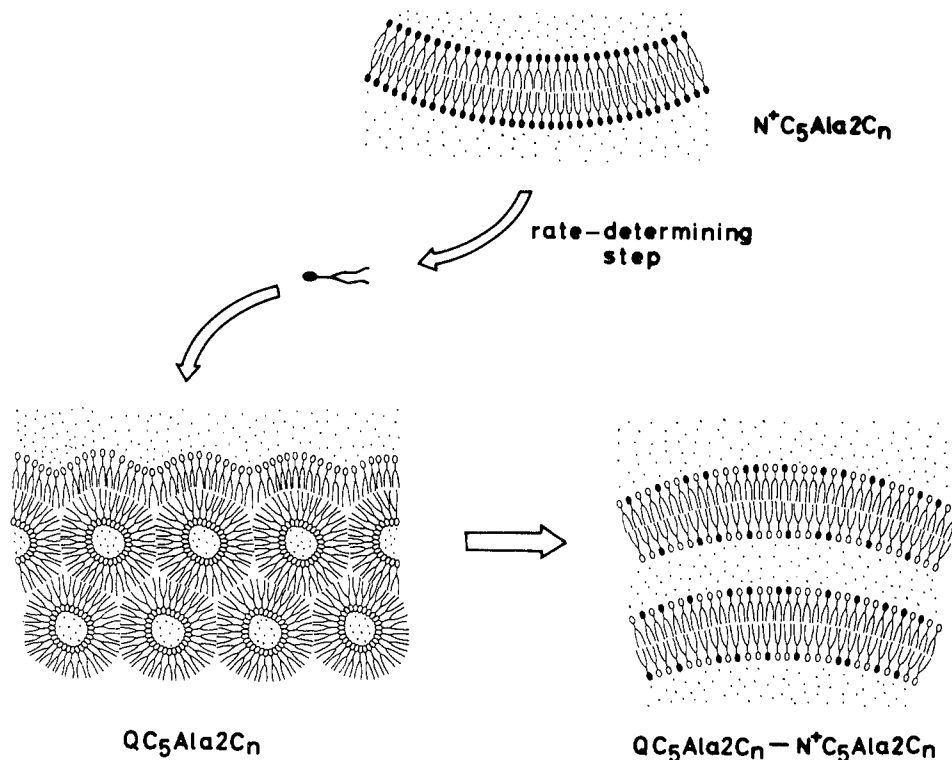


Figure 8. Schematic representation for morphological change of the QC_5Ala2C_n aggregate as induced by intermembrane interaction with the $N^+C_5Ala2C_n$ membrane.

logical change in a similar dynamic process.

The time scale of the morphological change evaluated by the turbidity change is well correlated with that observed by DSC. An incubation of an equimolar mixture of aqueous dispersions of $N^+C_5Ala2C_{14}$ and QC_5Ala2C_{16} (2.5 mM each) at 40.0 °C caused a rapid change of the DSC thermogram to give a new peak in the region lying between the original peaks of the individual aggregates within 1 h (Figure 7). On the other hand, the corresponding change of the DSC thermogram was completed in about 1 week for an equimolar mixture of aqueous dispersions of $N^+C_5Ala2C_{16}$ and QC_5Ala2C_{14} (2.5 mM each).⁶ Thus, the morphological change was evidently induced by the intermembrane lipid transfer between the aggregates composed of $N^+C_5Ala2C_n$ and those of QC_5Ala2C_n .

The intermembrane lipid transfer has been suggested to occur either through the intervening aqueous phase or by a process involving membrane collision.¹⁸ It has been reported that hydrophobic fluorescent molecules bearing the pyrenyl moiety are spontaneously transferred between single-walled bilayer vesicles of phosphatidylcholine through the bulk aqueous phase and the incremental free energy of activation for the fluorescent probes bearing polar moieties (alcohols, carboxylic acids, and their methyl esters) is ca. 740 cal/methylene unit.¹⁹ In addition, a good correlation was found to exist between the free energy of activation for the intermembrane transfer and the free energy of molecular transfer from a hydrophobic environment to the aqueous phase.²⁰ Consequently, the rate of intermembrane transfer is a function

Table II. Effect of Lipid Concentrations on the Morphological Change of Aggregates Individually Composed of $N^+C_5Ala2C_{14}$ and QC_5Ala2C_n ($n = 14$ and 16) at pH 7.0 and 21.5 °C

lipid concn, ^a M	half time, ^b min	
	$N^+C_5Ala2C_{14}$ + QC_5Ala2C_{14}	$N^+C_5Ala2C_{14}$ + QC_5Ala2C_{16}
6.25×10^{-4}	27	
5.00×10^{-4}	24	
4.15×10^{-4}	25	25
2.50×10^{-4}	21	24
1.25×10^{-4}	15	23

^a Identical concentrations for $N^+C_5Ala2C_{14}$ and QC_5Ala2C_n .
^b Evaluated from turbidity decrease at 400 nm.

of hydrophobicity of the transferred species. In light of the above information, the difference in hydrophobicity by four methylene units between the $N^+C_5Ala2C_n$ lipids (difference in the n value by 2) must be reflected on the difference in transfer rate by ca. 120-fold at 40.0 °C on the basis of the correlation $\Delta\Delta G^\ddagger = -RT \ln(k_1/k_2)$, where k_1 and k_2 stand for the rates of transfer of the two different cationic lipids. The rate differences obtained from Figure 6 are well in agreement with this value. Furthermore, the rate of morphological change does not depend on the hydrophobic nature of the nonionic lipids, QC_5Ala2C_{14} or QC_5Ala2C_{16} . If the morphological change takes place via a collision mechanism, the rate must be raised with an increase in concentrations of both lipids involved. However, within a range of experimental error, the rate of the turbidity change was independent of the lipid concentrations (Table II). The present results strongly indicate that the morphological change is induced by the one-way intermembrane transfer of the cationic lipid molecules through the intervening aqueous phase and the rate-determining step is referred to the diffusion of the cationic lipid molecules from the bilayer phase to the bulk aqueous phase.

In conclusion, the mechanism of morphological change induced by intermembrane interaction of synthetic peptide lipids individually bearing ionic and nonionic head groups can be drawn schematically as shown in Figure 8. The aggregates composed of QC_5Ala2C_n in aqueous media in the neutral pH region, which are regarded to have a unique bilayer structure, undergo mor-

(18) (a) Martin, F. J.; MacDonald, R. C. *Biochemistry* **1976**, *15*, 321–327. (b) Doody, M. C.; Pownall, H. J.; Kao, Y. J.; Smith, L. C. *Biochemistry* **1980**, *19*, 108–116. (c) Roseman, M. A.; Thompson, T. E. *Biochemistry* **1980**, *19*, 439–444. (d) Nichols, J. W.; Pagano, R. E. *Biochemistry* **1981**, *20*, 2783–2789. (e) McLean, L. R.; Phillips, M. C. *Biochemistry* **1981**, *20*, 2893–2900. (f) Papahadjopoulos, D.; Hui, S.; Vail, W. T.; Poste, G. *Biochim. Biophys. Acta* **1976**, *448*, 245–264. (g) Duckwitz-Peterlein, G.; Eilenberger, G.; Overath, P. *Biochim. Biophys. Acta* **1977**, *469*, 311–325. (h) Kremer, J. M. H.; Kops-Werkhoven, M. M.; Pathmamanoharan, C.; Gijzeman, O. L. J.; Wiersma, P. H. *Biochim. Biophys. Acta* **1977**, *471*, 177–188. (i) Maeda, T.; Ohnishi, S. *Biochem. Biophys. Res. Commun.* **1974**, *60*, 1509–1516.

(19) Pownall, H. J.; Hickson, D. L.; Smith, L. C. *J. Am. Chem. Soc.* **1983**, *105*, 2440–2445.

(20) Tanford, C. "The Hydrophobic Effect: Formation of Micelles and Biological Membranes"; Wiley: New York, 1973.

phological change to afford the normal bilayer membranes upon incubation with the bilayer aggregates composed of ionic peptide lipids $N^+C_5Ala2C_n$ and $(SO_3^-)C_5Ala2C_n$. The transfer of the ionic lipid molecules involved in the bilayer membranes to the QC_5Ala2C_n aggregates occurs through the intervening aqueous phase. The ionic lipid molecules invaded into the aggregates of QC_5Ala2C_n may act to break down the strong intermolecular

hydrogen-bonding interaction between the quinoyl moieties of the nonionic lipids and lead to the formation of the normal bilayer membranes.

Acknowledgment. The present work was supported in part by a Grant-in-Aid for Scientific Research from the Ministry of Education, Science, and Culture of Japan (No. 58430016).

Absorption and MCD Spectral Studies of the Decaammine(μ -dinitrogen- N',N')diosmium(5+) Mixed-Valence Ion

Lucjan Dubicki,[†] James Ferguson,^{*†} Elmars R. Krausz,[†] Peter A. Lay,[†] Marcel Maeder,[†] Roy H. Magnuson,[†] and Henry Taube^{*†}

Contribution from the Research School of Chemistry, Australian National University, Canberra, A.C.T., 2601, Australia, and the Department of Chemistry, Stanford University, Stanford, California 94305. Received May 22, 1984

Abstract: The red and near-infrared absorption and MCD spectra of the title compound have been measured over a range of temperature in KCl disks and poly(vinyl alcohol) (PVA). The two most intense bands, near 5500 and 14 300 cm^{-1} , have MCD C terms of opposite sign. A "single-ion" band whose energy is determined dominantly by spin-orbit coupling on osmium(III) occurs at 4700 cm^{-1} . Two other weaker absorptions appear near 8200 and 16 000 cm^{-1} . All of these bands have been interpreted by using a simple coupled chromophore model in which degeneracies are removed by a one-electron-transfer integral that models π bonding via the dinitrogen bridging ligand, between the d_{xz} and d_{yz} orbitals on each metal ion. Also essential to this model is the inclusion of both spin-orbit coupling on the metal centers and the tetragonal field due to the dinitrogen bridge via an effective Hamiltonian treatment. Allowed electric dipole absorption intensities have been formulated in terms of effective electric dipole transition matrix elements. These are determined by the odd-parity components associated with the C_{4v} site symmetry of each metal center within the dimer. The model is consistent with a qualitative MO description that includes spin-orbit coupling.

Although the first dinitrogen-bridged complex, $[(NH_3)_5RuN_2Ru(NH_3)_5]^{4+}$, was reported in 1968,¹ spectroscopic properties of the corresponding mixed-valence (5+) ion were reported only very recently along with the Os analogue.² Apart from the interest in these complexes from the viewpoint of N_2 fixation,² the osmium complex was the first example of a stable mixed-valence ion that has both high symmetry (D_{4h}) and more than one atom in the bridge between the two metal centers. Its stability and symmetry are, of course, most attractive for spectroscopic measurements and allow a direct comparison with the much studied pyrazine-bridged complexes having D_{2h} symmetry.³ Studies of these latter complexes have been seminal in the formation of several models of mixed-valence "delocalization",⁴ but the situation is not clearly resolved even in the most recent calculations.⁵

A simple MO scheme without spin-orbit coupling² cannot give a quantitative description of the observed spectra. We have used an effective Hamiltonian model,⁶ essentially a valence-bond method, that is more convenient for the calculation of transition intensities and for the inclusion of spin-orbit coupling. This paper reports the absorption and MCD of the title compound, together with a theoretical analysis.

Octahedral Os(III), having a hole in the t_2 shell, has only a single term of T_2 symmetry which is also well separated from others associated with other electronic configurations (e_g and charge transfer) so that an effective Hamiltonian model is very well suited for the analysis of spin-orbit and low-symmetry effects in the monomer case. The same approach can be used for symmetric dimers by including an interion coupling term in the effective Hamiltonian. We have developed such a model⁷ for the well-known mixed-valence ruthenium Creutz-Taube dimer and the corresponding osmium ion.⁸ Whereas the metal ions in the pyrazine dimer have C_{2v} symmetry, so that the μ -dinitrogen-diosmium ion is C_{4v} and the symmetric dimer has D_{4h} symmetry.

This change to 4-fold symmetry produces significant differences in the calculated energy level patterns which are borne out by analyses of the absorption spectrum and the corresponding MCD of the title compound.

MCD Spectroscopy

MCD spectroscopy⁹ is a very powerful method in the assignment of absorption spectra of transition-metal-ion complexes. It has been used to analyze the near-infrared spectra of pentaamine complexes of Os(III) with π -bonding ligands.¹⁰

MCD spectroscopy has recently been introduced to the study of mixed-valence compounds.^{7,11} Mixed-valence compounds most often have dominant linear (interion) polarization of absorption. This is easily understood as intensity arises fundamentally from the transfer of an electron from one metal center to the other, even in the case of strongly coupled symmetric systems! In the recent extensive MO calculations of Ondrechen et al.,⁵ the characteristic transition in the Creutz-Taube complex is reaffirmed

(1) Harrison, D. E.; Weisberger, E.; Taube, H. *Science (Washington, D.C.)* **1968**, *159*, 320-322.

(2) Richardson, D. E.; Sen, J. P.; Buhr, J. D.; Taube, H. *Inorg. Chem.* **1982**, *21*, 3136-3140.

(3) Creutz, C. *Prog. Inorg. Chem.* **1983**, *30*, 1-73.

(4) Brown, D. M., Ed. "Mixed-Valence Compounds"; Reidel: Dordrecht, Holland, 1980.

(5) Ondrechen, M. J.; Ellis, D. E.; Ratner, M. A. *Chem. Phys. Lett.* **1984**, *109*, 50-55.

(6) Sugano, S.; Tanabe, Y.; Kamimura, H. "Multiplets of Transition-Metal Ions in Crystals"; Academic Press: New York, 1970.

(7) Dubicki, L.; Ferguson, J.; Krausz, E. R. *J. Am. Chem. Soc.* **1985**, *107*, 179-182.

(8) Magnuson, R. H.; Lay, P. A.; Taube, H. *J. Am. Chem. Soc.* **1983**, *105*, 2507-2509.

(9) Piepho, S. B.; Schatz, P. N. "Group Theory in Spectroscopy"; Wiley: New York, 1983.

(10) Dubicki, L.; Ferguson, J.; Krausz, E. R.; Lay, P. A.; Maeder, M.; Taube, H. *J. Phys. Chem.* **1984**, *88*, 3940-3941.

(11) Krausz, E. R.; Ludi, A. *Inorg. Chem.*, in press.

[†] Australian National University.

^{*} Stanford University.